The CDK5 repressor CDK5RAP1 is a methylthiotransferase acting on nuclear and mitochondrial RNA

Veronika Reiter, Dorothea M.S. Matschkal, Mirko Wagner, Daniel Globisch, Andrea C. Kneuttinger, Markus Müller* and Thomas Carell*

Center for Integrated Protein Science Munich (CIPSM), Department of Chemistry, Ludwig-Maximilians University, Munich 81377, Germany

ABSTRACT

The unusual cyclin-dependent protein kinase 5 (CDK5) was discovered based on its sequence homology to cell cycle regulating CDKs. CDK5 was found to be active in brain tissues, where it is not involved in cell cycle regulation but in the regulation of neuronal cell differentiation and neurocytoskeleton dynamics. An aberrant regulation of CDK5 leads to the development of various neurodegenerative diseases including Alzheimer's disease. Although CDK5 is not regulated by cyclins, its activity does depend on the association with a protein activator and the presence or absence of further inhibitory factors. Recently, CDK5RAP1 was discovered to inhibit the active CDK5 kinase. Here, we show that CDK5RAP1 is a radical SAM enzyme, which postsynthetically converts the RNA modification N6-isopentenyladenosine (i^{6}A) into 2-methylthio-N6-isopentenyladenosine (ms^{2}i^{6}A). This conversion is surprisingly not limited to mitochondrial tRNA, where the modification was known to exist. Instead, CDK5RAP1 introduces the modification also into nuclear RNA species establishing a link between postsynthetic kinase-based protein modification and postsynthetic RNA modification.

INTRODUCTION

Cyclin-dependent protein kinase 5 (CDK5) is an atypical CDK which has no function in cell-cycle progression and does not require cyclin interaction for its activity. Instead, CDK5 has its major function in the organization of the cytoarchitecture of the central nervous system (CNS) (1). The kinase activity is regulated by the proteins p35 (CDK5R1) and p39 (CDK5R2) or their truncated forms p25 and p29, respectively (2). These regulatory subunits are mainly expressed in brain tissue, while CDK5 itself plays a role in various other tissues as well. In the brain, CDK5 is involved in neuronal development and neurogenesis (3). Its aberrant regulation leads to neurodegenerative diseases like Alzheimer's and Parkinson's disease. In Alzheimer's disease, for example, CDK5 is hyperactivated by tight binding to a proteolytically truncated version of the regulator CDK5R1, p25. This in turn leads to aberrant phosphorylation of the tau protein, which then undergoes detrimental fibrillation (4). The tight regulation of CDK5R1 is consequently of paramount importance. While three interaction partners of CDK5R1 were identified in a yeast-two-hybrid screen in 2000 (5), only one of these proteins (C42) was shown to inhibit CDK5 activity by preventing the formation of the activated complex (6). Recently, it was suggested that C42 (later renamed CDK5 regulatory subunit associated protein 1, CDK5RAP1) is a radical SAM enzyme (7) with homology to the bacterial MiaB protein (8), which introduces a methylthio-group into N6-isopentenyladenosine in tRNA at position A37, next to the anticodon (9,10) (Supplementary Scheme S1). The resulting hypermodified adenine, 2-methylthio-N6-isopentenyladenosine (ms^{2}i^{6}A) functions in codon suppression (11) and stabilization of the codon/anticodon interaction (12). The biochemical link established by CDK5RAP1 between the enzymatic modification of tRNA anticodon loops and CDK5 kinase activity is highly unusual, particularly because the modified base ms^{2}i^{6}A is known to exist in tRNA of

procaryotic origin (10). In mammals it is hence expected to occur only in mitochondrial tRNA, where it is found in tRNA^{Trp}, tRNA^{Phe} and tRNA^{Tyr} (13). Indeed, we recently confirmed that only traces of ms^{2}i^{6}A are present in cytosolic tRNA, while it is very abundant in mitochondrial tRNA (14).

MATERIALS AND METHODS

Subcellular localization

GFP-reporter plasmids for the subcellular localization of the human CDK5RAP1 variants were obtained from Origene (RG216600 and RG208724). HeLa cells were grown at 37°C and 5% CO$_2$ in RPMI 1640 medium supplemented with 10% (v/v) fetal bovine serum and 0.1% antibiotic/antimycotic (Gibco). Splitting was performed at 80% confluence. For transfection, 1.5×10^4 cells/300 μl were seeded in an 8-well plate (μslide, IBIDI) with 1 cm^2 surface area. After 24 h, the cells were transfected with 25 μl *jetPrime* reaction mix (Peqlab) containing 250 ng plasmid DNA. After 4 h, the medium was exchanged. Forty-eight hours after transfection, the cells were visualized on a Leica TCS SPE confocal microscope at 488- (GFP) and 532 nm excitation for MitoTracker Red (Molecular Probes) to visualize the mitochondria.

Immunocytochemistry

The growth conditions were essentially the same as described earlier, except that a 16-well plate (Chamber slide, Thermo Fisher Scientific) was seeded with 1.0×10^3 cells/150 μl. After 24 h, the cells were fixed for 15 min in 4% fresh PFA solution [4% (w/v) paraformaldehyde dissolved at 70°C in PBS]. After three 10-min washing steps in PBS, the cells were incubated over night with rabbit anti-CDK5RAP1 (SAB2105127, Sigma-Aldrich) 1:300 in PBS supplemented with 0.3% Triton X-100 and 5% Chemiblocker (Millipore). The cells were washed three times 5 min in PBS and incubated with Alexa488-conjugated anti-rabbit IgG F(ab′)2 fragment (Cell Signaling) 1:750 in PBS containing 2% Chemiblocker for 1.5 h. After two washing steps, the cells were immersed for 5 min in PBS containing 0.4 μg/ml propidium iodide (Sigma-Aldrich). For co-staining of CDK5, mouse anti-CDK5 (C6118, Sigma-Aldrich) was added at 1:300 dilution and visualized with Alexa555-conjugated anti-mouse IgG F(ab′)2 fragment (Cell Signaling). The slides were mounted in Fluoromount G (Beckman Coulter) and analyzed on a Leica TCS SPE confocal microscope.

Cytochrome C oxidase assay

The respiratory activity of mitochondria in whole cell lysates of pork tissue was measured using the Cytochrome C Oxidase Assay Kit of Sigma-Aldrich. The tissue samples (200 mg) were homogenized with 450 μl ice-cold PBS at 30 Hz for 2 min with a tissue lyser (Qiagen). Subsequently, 50 μl of 10 mM maltoside was added and the lysis solution was shaken at 4–9°C for at least 15 min. The mixture was centrifuged at 4°C, 16 000 × g for 10 min and the supernatant was diluted 10-fold in enzyme dilution buffer. Measurements and analysis of the data took place according to the manufacturer. The mean values in nmol/(min × ml) (= 1 mU) were eventually divided by the total protein concentration of the cell lysates determined using the Bradford assay. The enzyme activity is shown in nmol/(min × mg protein).

Complementation assay

The bacterial expression construct of the shorter CDK5RAP1 variant 2 was obtained by PCR amplification from the human cDNA ORF Clone (Origene, RG216600) using Phusion High-Fidelity DNA polymerase (NEB) with the two primers 5′-CACCATGATGGAT GAACTTCTTGGAAGGC-3′ and 5′-TCAGCAATATG CAGAAGAGTCCCTCAGAG-3′. The 1498-bp PCR product was cloned in a two-step Gateway reaction via the vector pENTR/TEV/D-TOPO (Invitrogen) into the expression vector pDEST007 (15), which results in the addition of an N-terminal *Strep-Tag II* (IBA). To exclude effects of protein overexpression and antibiotic selection, all strains were transformed with the same plasmid backbone, encoding either human CDK5RAP1-v2 or the unrelated protein BstPOL I (control). We used the wild-type strain BW25113 as well as the deletion mutant *ΔmiaB* (JW0658) from the Keio Collection, NBRP (NIG, Japan) (16). All deletions were PCR-verified. The cells were grown under 100 μg/ml carbenicillin selection and the deletions were further selected with 50 μg/ml kanamycin at 37°C, while shaking at 200 rpm in 1 l of LB-medium until OD$_{600}$ = 0.6 was reached. The expression of CDK5RAP1-v2 and the control protein was induced by addition of 200 μg anhydrotetracycline and the incubation was continued at 16°C for 12 h. Cells were harvested (10 000 × g, 8 min, 4°C) and stored at −20°C until RNA preparation.

siRNA knockdown

The growth conditions were essentially the same as described for the subcellular localization, except that a 75-cm^2 tissue culture flask was seeded with 1.5×10^6 cells. After 24 h, the cells were transfected with 4 μg of endonuclease-derived siRNA (esiRNA, esiMission CDK5RAP1, Sigma-Aldrich) or the same amount of an unrelated esiRNA (esiMission EGFP, Sigma-Aldrich). Twenty-four hour post-transfection, the medium was exchanged and HeLa cells were transfected again as described earlier. Twenty-four hours after the second transfection, the medium was exchanged. Total RNA was extracted after 72 h as described below.

RNA isolation

Total RNA was prepared with the Trifast reagent from Peqlab. tRNA was isolated according to our established method (17). The isolation of mRNA followed the mTRAP Maxi Kit from Active Motif. rRNA was obtained via the enrichment of ribosomes. For the preparation of small RNA, the mirPremier-Kit (Sigma Aldrich) was used. For detailed information, see Supplementary Methods.
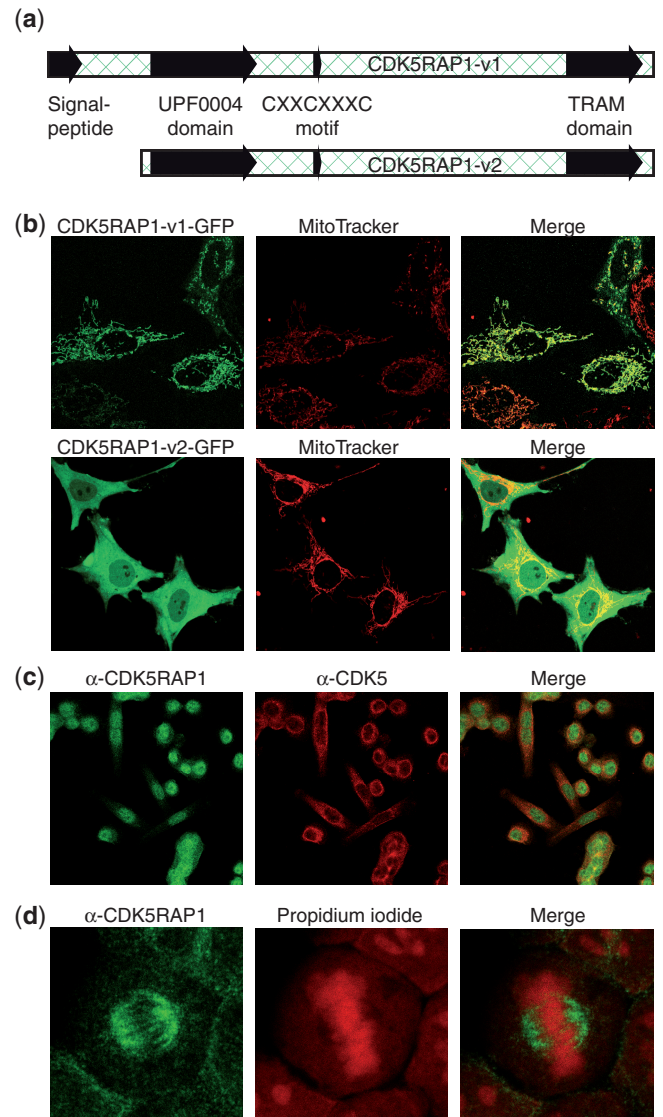
RESULTS

Subcellular localization of CDK5RAP1

In order to unravel the unusual link between CDK5 kinase activity and RNA modification chemistry, we investigated the catalytic properties and the cellular distribution of CDK5RAP1, which exists in different splice variants (18). Variant 1 contains an N-terminal extension that is by computational methods predicted to comprise a mitochondrial import signal (score = 0.647, TargetP1.1) (19), while variant 2 lacks this extension (Figure 1a). To analyze the subcellular distribution of both splicing variants, we transfected HeLa cells with GFP fusions of these two CDK5RAP1 splice variants. The confocal analysis clearly shows a mitochondrial localization of variant 1. In order to secure the interpretation we performed a colocalization with a mitochondrial counterstain and indeed observed the colocalization of variant 1 and the MitoTracker (Figure 1b). Variant 2, which is lacking the putative import signal, we found distributed in both cytoplasm and nucleus, respectively (Figure 1b), with the stronger signal appearing in the cytoplasm. This distribution was confirmed by immunocytochemical (ICC) staining of CDK5RAP1, however with a stronger preference for nuclear localization (Figure 1c). Interestingly, in both live-cell imaging and ICC methods, CDK5RAP1 appeared to be excluded from the nucleoli. This is a somehow surprising observation since the nucleoli are the compartment where RNA processing mainly occurs. ICC staining with an antibody against CDK5 showed that there is no apparent colocalization of CDK5 with CDK5RAP1 (Figure 1c). This is in accordance with CDK5RAP1s mode of CDK5-inhibition by preventing formation of the activated CDK5 complex. In some cells, CDK5RAP1 shows an association with the mitotic spindle (Figure 1d). Such localization was previously shown also for CDK5RAP2 (20), the second CDK5R1-binding protein identified in the yeast two hybrid screen. This result suggests that CDK5RAP1 might be interacting with cell cycle regulating mitotic CDKs as well. The mitochondrial localization of CDK5RAP1 variant 1 is in full agreement with the suggested MiaB-like function in ms^2i^6A biosynthesis in mitochondrial tRNA.
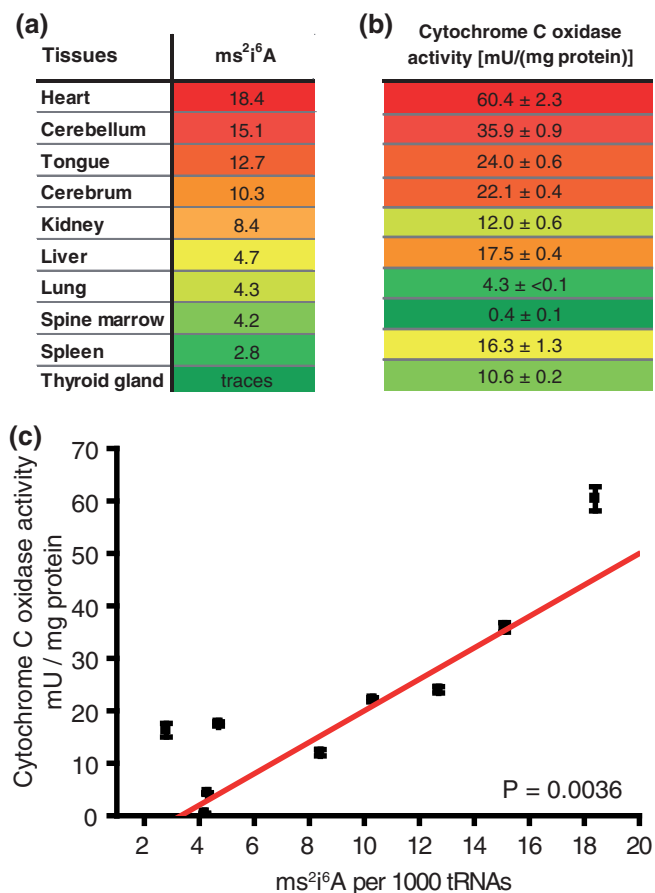
Occurrence of ms^2i^6A in mitochondrial tRNA

The presence of ms^2i^6A in mitochondrial tRNA was shown previously (21), and we have further verified its localization. In order to investigate the role of ms^2i^6A for mitochondrial activity, we isolated tRNA from various pork tissues, fully digested these RNA fractions and analyzed the nucleoside mixture by LC-MS (Supplementary Methods). Precise quantification of ms^2i^6A in these lysates was enabled by adding a synthetic, isotope-labeled ms^2i^6A standard to the mixture as described recently by us in detail (17). As a marker for mitochondrial activity, we quantified the activity of cytochrome C oxidase (COX). The results summarized in Figure 2 clearly show a strong correlation with mitochondrial activity. Tissues with a high-energy demand like muscle and brain tissue feature also the highest

(a)

Signal-peptide   UPF0004 domain   CXXCXXXC motif   CDK5RAP1-v1   TRAM domain

CDK5RAP1-v2

(b) CDK5RAP1-v1-GFP   MitoTracker   Merge

CDK5RAP1-v2-GFP   MitoTracker   Merge

(c) α-CDK5RAP1   α-CDK5   Merge

(d) α-CDK5RAP1   Propidium iodide   Merge

Figure 1. Subcelluar distribution of CDK5RAP1 variants. (**a**) Representation of the two investigated CDK5RAP1 variants with mitochondrial import sequence and catalytic domain. (**b**) Live-cell images of HeLa cells transfected with C-terminally GFP-tagged CDK5RAP1-v1 and CDK5RAP1-v2. For the counterstain of mitochondria, cells were incubated with MitoTracker Red dye. The merge shows that CDK5RAP1-v1 colocalizes with mitochondria, while CDK5RAP1-v2 is distributed in both cytoplasm and nucleus. (**c**) Formaldehyde-fixed HeLa cells were stained with an antibody against the N-terminal region of CDK5RAP1-v2 (Alexa-488, green) and against CDK5 (Alexa-555, red). The localization of CDK5RAP1 is predominantly nuclear with little overlap to CDK5. (**d**) Again, fixed HeLa cells were stained with anti-CDK5RAP1 (green). For localization of nucleic acids, propidium iodide (red) was used. CDK5RAP1 shows an association with the mitotic spindle.

concentrations of ms^2i^6A. We further enriched mitochondria from porcine heart and quantified ms^2i^6A in both mitochondrial and cytosolic tRNA. A strong enrichment was achieved in preparations of mitochondria (80 modifications per 1000 tRNA) as compared to cytosolic tRNA (6 per 1000). Residual ms^2i^6A in these preparations likely originates from ruptured mitochondria. This data is taken from Ref. (14).

(a)

Tissues	ms^2i^6A
Heart	18.4
Cerebellum	15.1
Tongue	12.7
Cerebrum	10.3
Kidney	8.4
Liver	4.7
Lung	4.3
Spine marrow	4.2
Spleen	2.8
Thyroid gland	traces

(b)

Cytochrome C oxidase activity [mU/(mg protein)]
60.4 ± 2.3
35.9 ± 0.9
24.0 ± 0.6
22.1 ± 0.4
12.0 ± 0.6
17.5 ± 0.4
4.3 ± <0.1
0.4 ± 0.1
16.3 ± 1.3
10.6 ± 0.2

(c)

Figure 2. Correlation of ms^2i^6A content with mitochondrial activity. (**a**) Content of ms^2i^6A in tRNA of various pork tissues, sorted by descending amount. Highest values in red, lowest in green. (**b**) Cytochrome C oxidase activity in the same tissues. For comparison, the same color code was used. (**c**) Correlation plot of COX activity versus ms^2i^6A content.

Occurrence of ms^2i^6A in nuclear RNA

Based on this data, we reasoned that the nucleocytoplasmic localization of variant 2 of CDK5RAP1 causes the transformation of i^6A into ms^2i^6A in nuclear RNA species as well, where ms^2i^6A was not observed so far. We applied our isotope-based quantification method on preparations of various RNA species (Figure 3a). In agreement with our earlier data and with the Warburg effect, which describes strongly impaired mitochondrial function in cancer cells, we were unable to detect significant amounts of ms^2i^6A in the total tRNA fraction of HeLa cells (17). Also, the ribosomal RNA, which was obtained from ribosome-enriched preparations, did contain only traces of ms^2i^6A. In contrast, polyadenylated RNA enriched by oligo-dT hybridization gave a significant signal for ms^2i^6A (Figure 3b). The amount of the precursor i^6A in polyA-RNA is very low, showing that in this RNA species full conversion to ms^2i^6A occurs (Figure 3c). The highest amount of ms^2i^6A was found in preparations of small RNA, using a commercial miRNA preparation kit. These preparations contain next to tRNA (~70–100 nt) also RNA species of a larger size (Supplementary Figure S1). The presence of tRNA is reflected by the high i^6A content observed, similar to that seen in preparations of tRNA. By exclusion of ribosomal and transfer RNA as the source of ms^2i^6A, we reason that ms^2i^6A is indeed an RNA modification that next to mitochondrial tRNA exists also in a yet unidentified nuclear RNA species. The data prove that ms^2i^6A is far more wide spread than thought until today.

### CDK5RAP1 is an N6-isopentenyladenosine methylthiotransferase

In order to proof that the CDK5 inhibitory protein CDK5RAP1 is responsible for the biosynthesis of ms^2i^6A in RNA (Supplementary Scheme S1), we expressed variant 2, which is lacking the mitochondrial import sequence, in a MiaB-deficient *Escherichia coli* strain from the Keio collection (16) and analyzed the ms^2i^6A content in tRNA by mass spectrometry. Although the protein turned out to be rather insoluble (Supplementary Figure S2), we detected significantly elevated levels of ms^2i^6A in the complemented cells (Figure 4a), showing that CDK5RAP1 has indeed MiaB-like catalytic properties. To address the possibility that bacterial tRNA is a bad substrate for human CDK5RAP1, we measured also the ms^2i^6A content of total RNA and received the same results, however with less pronounced differences (Supplementary Figure S3). We could further exclude the possibility that CDK5RAP1 generates ms^2t^6A. Whereas t^6A is present in *E. coli* in significant amounts, ms^2t^6A remains undetectable even after CDK5RAP1 overexpression (Supplementary Figure S4b). To further verify that CDK5RAP1 is the responsible enzyme for the synthesis of the detected ms^2i^6A in RNA extracts from HeLa cells, we next measured ms^2i^6A levels in HeLa cells after knockdown of CDK5RAP1 by transfection with endonuclease-derived siRNA (esiRNA), targeting both variants. Transfection with esiRNA resulted indeed in a 78% decrease of ms^2i^6A content after 72 h in comparison to cells treated with esiRNA against green fluorescent protein (Figure 4b). Again, the content of ms^2t^6A is not affected by knockdown of CDK5RAP1, proving that t^6A is not recognized as a substrate of CDK5RAP1 (Supplementary Figure S4a). The amount of m^6A served in this study as an internal reference in both experiments and did not show significant alterations. From this study, we can conclude that the ms^2i^6A found in RNA of HeLa cells is generated by the action of CDK5RAP1.

DISCUSSION

Our study provides a direct link between posttranslational protein modification processes such as phosphorylations catalyzed by CDK5 and the processes that implement posttranscriptional RNA modifications. Furthermore, we show that nuclear RNA modifications are not limited to rather small modifications such as methylation or A-to-I editing (22), but that the modifications involve also the introduction of unusual hypermodified bases such as
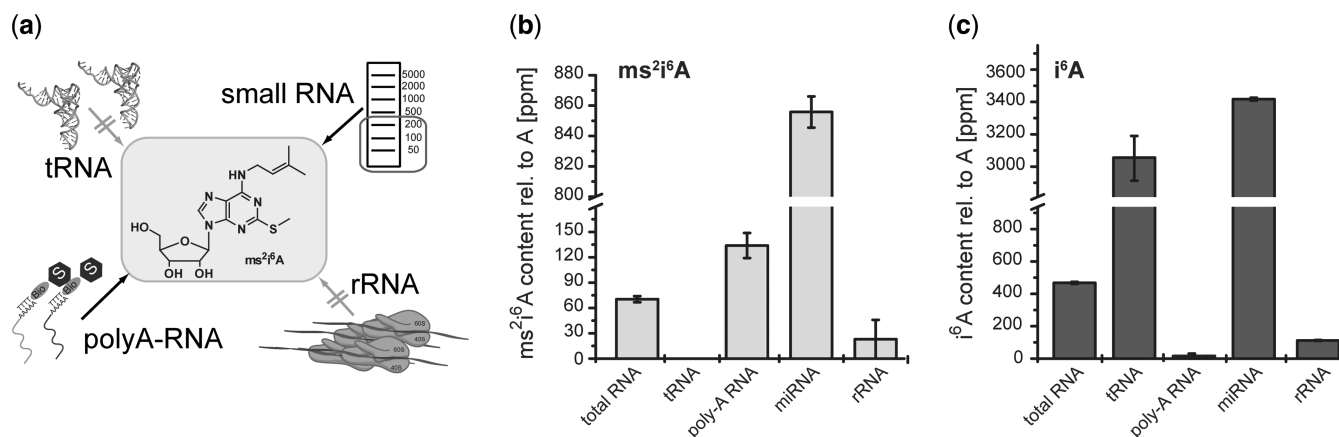
Figure 3. ms^2i^6A/i^6A content in different RNA species of HeLa cells. (**a**) Overview of investigated RNA fractions. (**b**) ms^2i^6A content in different RNA species of HeLa cells relative to unmodified adenosine (ppm). tRNA and rRNA contain no or only trace amounts of ms^2i^6A. However we found ms^2i^6A to be enriched in polyA-RNA and even higher in miRNA. (**c**) i^6A content in different RNA species of HeLa cells relative to adenosine (ppm). tRNA and miRNA contain high amounts of i^6A. In polyA-RNA and rRNA, i^6A is only present in traces or low amounts.
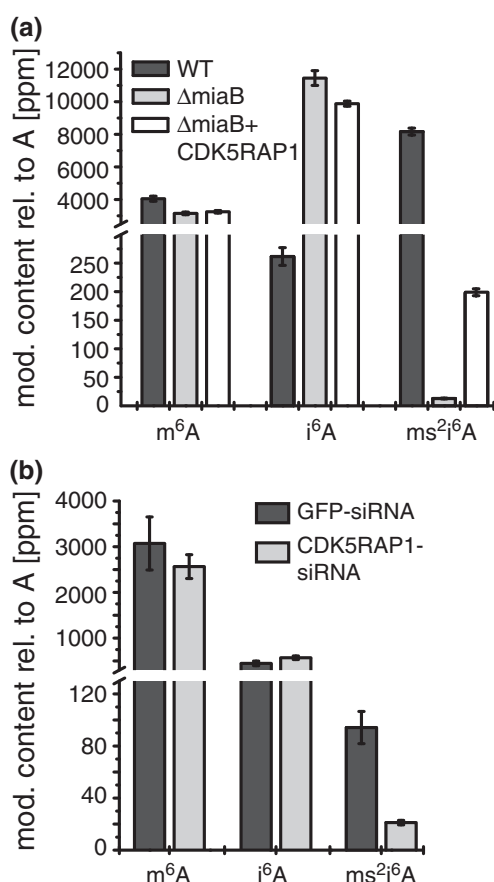
Figure 4. CDK5RAP1 is the human homolog of the bacterial protein MiaB. (**a**) Complementation assay in *E. coli.* Quantification of m^6A, i^6A and ms^2i^6A in tRNA of wild-type *E. coli*, a MiaB-deficient strain and a MiaB-deficient strain complemented with CDK5RAP1. m^6A was used as internal standard and levels did not change during the experiment. i^6A level increased in ΔMiaB and compared to WT, because of lack of conversion to ms^2i^6A. ΔMiaB+CDK5RAP1 shows a decreased i^6A level in comparison to ΔMiaB, generated by the complementation. By the expression of CDK5RAP1, the ms^2i^6A level increases 15-fold in comparison to ΔMiaB. (**b**) siRNA knockdown in HeLa cells. Cells were transfected twice with esiRNA against CDK5RAP1. Non-coding esiRNA against EGFP served as a control. After 72 h, total RNA was extracted and the modification content was determined by LC-MS. m^6A and i^6A remain constant, while ms^2i^6A decreased ~78%.

ms^2i^6A. We present the biosynthetic enzyme CDK5RAP1, which has a dual role as RNA methylthiotransferase and inhibitor of CDK5. We further find differential localization of the two splicing variants of CDK5RAP1 to mitochondria and cytosol. Alternative splicing could therefore regulate the dual function of this enzyme. The involvement of RNA modifying enzymes in other developmental or metabolic processes is a new concept that gained recently support by two other observations. First, CDKAL1, which is a long-known factor in typ II diabetes (T2D) and a close homolog of CDK5RAP1, was characterized as an N6-threonyladenosine (t^6A) methylthiotransferase. Despite the high homology to CDK5RAP1, which led to its name, CDKAL1 does not accept i^6A as a substrate (23). Further it was shown to localize in the endoplasmatic reticulum (ER) with the C-terminus being the determinant for this localization (24). While t^6A occurs in mitochondrial tRNA just as i^6A, its methylthiolated species ms^2t^6A was not found in mitochondrial tRNA species and appears to be restricted to the anticodon loop of tRNA^{Lys} (http://trnadb.bioinf.uni-leipzig.de/) (13). The second example that connects RNA modifications with lifestyle disease, is the fat and obesity associated protein FTO, which was discovered in 2007 to be an iron(II) and 2-oxoglutarate dependent demethylase (25). Just recently it was found that FTO is able to demethylate m^6A, which is an important and highly abundant modification in mRNA. FTO co-localizes with the splicing factor SC35 in the nucleus, where it was suggested to have a role in regulation of splicing (26). Our results now show that RNA modification is connected to the regulation of a critical kinase (CDK5) involved in neuronal cell differentiation. We believe that the introduction of ms^2i^6A into RNA will strongly influence the function of the RNA species. ms^2i^6A is a modification which strongly alters the RNA structure and duplex stability (27) and influences for example codon recognition by stacking interactions with neighboring RNA duplexes (12). The ability of the base to stabilize loop structures can serve multiple purposes in many RNA species. It can alter for example the specific

target binding of miRNA by duplex interaction, influence miRNA processing by perforation of the loop structure in pre-miRNA or it may aid in intron splicing.

SUPPLEMENTARY DATA

Supplementary Data are available at NAR Online: Supplementary Figures 1–4, Supplementary Methods, Supplementary Methods Figures 1–3 and Supplementary Scheme 1.

ACKNOWLEDGEMENTS

FUNDING

REFERENCES

1. Dhavan,R. and Tsai,L.H. (2001) A decade of CDK5. *Nat. Rev. Mol. Cell Biol.*, **2**, 749–759.
2. Liebl,J., Fürst,R., Vollmar,A.M. and Zahler,S. (2011) Twice switched at birth: cell cycle-independent roles of the "neuron-specific" cyclin-dependent kinase 5 (Cdk5) in non-neuronal cells. *Cell. Signal.*, **23**, 1698–1707.
3. Jessberger,S., Gage,F.H., Eisch,A.J. and Lagace,D.C. (2009) Making a neuron: Cdk5 in embryonic and adult neurogenesis. *Trends Neurosci.*, **32**, 575–582.
4. Gong,C.X. and Iqbal,K. (2008) Hyperphosphorylation of microtubule-associated protein tau: a promising therapeutic target for Alzheimer disease. *Curr. Med. Chem.*, **15**, 2321–2328.
5. Ching,Y.P., Qi,Z. and Wang,J.H. (2000) Cloning of three novel neuronal Cdk5 activator binding proteins. *Gene*, **242**, 285–294.
6. Ching,Y.P., Pang,A.S., Lam,W.H., Qi,R.Z. and Wang,J.H. (2002) Identification of a neuronal Cdk5 activator-binding protein as Cdk5 inhibitor. *J. Biol. Chem.*, **277**, 15237–15240.
7. Atta,M., Mulliez,E., Arragain,S., Forouhar,F., Hunt,J.F. and Fontecave,M. (2010) S-Adenosylmethionine-dependent radical-based modification of biological macromolecules. *Curr. Opin. Struct. Biol.*, **20**, 684–692.
8. Kaminska,K.H., Baraniak,U., Boniecki,M., Nowaczyk,K., Czerwoniec,A. and Bujnicki,J.M. (2008) Structural bioinformatics analysis of enzymes involved in the biosynthesis pathway of the hypermodified nucleoside ms(2)io(6)A37 in tRNA. *Proteins*, **70**, 1–18.
9. Pierrel,F., Douki,T., Fontecave,M. and Atta,M. (2004) MiaB protein is a bifunctional radical-S-adenosylmethionine enzyme involved in thiolation and methylation of tRNA. *J. Biol. Chem.*, **279**, 47555–47563.
10. Esberg,B., Leung,H.C., Tsui,H.C., Bjork,G.R. and Winkler,M.E. (1999) Identification of the miaB gene, involved in methylthiolation of isopentenylated A37 derivatives in the tRNA of Salmonella typhimurium and Escherichia coli. *J. Bacteriol.*, **181**, 7256–7265.
11. Bouadloun,F., Srichaiyo,T., Isaksson,L.A. and Bjork,G.R. (1986) Influence of modification next to the anticodon in tRNA on codon context sensitivity of translational suppression and accuracy. *J. Bacteriol.*, **166**, 1022–1027.
12. Jenner,L.B., Demeshkina,N., Yusupova,G. and Yusupov,M. (2010) Structural aspects of messenger RNA reading frame maintenance by the ribosome. *Nat. Struct. Mol. Biol.*, **17**, 555–560.
13. Sprinzl,M. and Vassilenko,K.S. (2005) Compilation of tRNA sequences and sequences of tRNA genes. *Nucleic Acids Res.*, **33**, D139–D140.
14. Globisch,D., Pearson,D., Hienzsch,A., Brückl,T., Wagner,M., Thoma,I., Thumbs,P., Reiter,V., Kneuttinger,A.C., Müller,M. et al. (2011) Systems-based analysis of modified tRNA bases. *Angew. Chem. Int. Ed. Engl.*, **50**, 9739–9742.
15. Ober,M., Müller,H., Pieck,C., Gierlich,J. and Carell,T. (2005) Base pairing and replicative processing of the formamidopyrimidine-dG DNA lesion. *J. Am. Chem. Soc.*, **127**, 18143–18149.
16. Baba,T., Ara,T., Hasegawa,M., Takai,Y., Okumura,Y., Baba,M., Datsenko,K.A., Tomita,M., Wanner,B.L. and Mori,H. (2006) Construction of Escherichia coli K-12 in-frame, single-gene knockout mutants: the Keio collection. *Mol. Syst. Biol.*, **2**, 1–11.
17. Brückl,T., Globisch,D., Wagner,M., Müller,M. and Carell,T. (2009) Parallel isotope-based quantification of modified tRNA nucleosides. *Angew. Chem. Int. Ed. Engl.*, **48**, 7932–7934.
18. Zou,X., Ji,C., Jin,F., Liu,J., Wu,M., Zheng,H., Wang,Y., Li,X., Xu,J., Gu,S. et al. (2004) Cloning, characterization and expression of CDK5RAP1_v3 and CDK5RAP1_v4, two novel splice variants of human CDK5RAP1. *Genes Genet. Syst.*, **79**, 177–182.
19. Emanuelsson,O., Brunak,S., von Heijne,G. and Nielsen,H. (2007) Locating proteins in the cell using TargetP, SignalP and related tools. *Nat. Protoc.*, **2**, 953–971.
20. Bond,J., Roberts,E., Springell,K., Lizarraga,S.B., Scott,S., Higgins,J., Hampshire,D.J., Morrison,E.E., Leal,G.F., Silva,E.O. et al. (2005) A centrosomal mechanism involving CDK5RAP2 and CENPJ controls brain size. *Nat. Genet.*, **37**, 353–355.
21. Sakurai,M., Ohtsuki,T., Suzuki,T. and Watanabe,K. (2005) Unusual usage of wobble modifications in mitochondrial tRNAs of the nematode Ascaris suum. *FEBS Lett.*, **579**, 2767–2772.
22. Knoop,V. (2011) When you can't trust the DNA: RNA editing changes transcript sequences. *Cell. Mol. Life Sci.*, **68**, 567–586.
23. Arragain,S., Handelman,S.K., Forouhar,F., Wei,F.Y., Tomizawa,K., Hunt,J.F., Douki,T., Fontecave,M., Mulliez,E. and Atta,M. (2010) Identification of eukaryotic and prokaryotic methylthiotransferase for biosynthesis of 2-methylthio-N6-threonylcarbamoyladenosine in tRNA. *J. Biol. Chem.*, **285**, 28425–28433.
24. Wei,F.Y., Suzuki,T., Watanabe,S., Kimura,S., Kaitsuka,T., Fujimura,A., Matsui,H., Atta,M., Michiue,H., Fontecave,M. et al. (2011) Deficit of tRNA(Lys) modification by Cdkal1 causes the development of type 2 diabetes in mice. *J. Clin. Invest.*, **121**, 3598–3608.
25. Gerken,T., Girard,C.A., Tung,Y.C., Webby,C.J., Saudek,V., Hewitson,K.S., Yeo,G.S., McDonough,M.A., Cunliffe,S., McNeill,L.A. et al. (2007) The obesity-associated FTO gene encodes a 2-oxoglutarate-dependent nucleic acid demethylase. *Science*, **318**, 1469–1472.
26. Jia,G., Fu,Y., Zhao,X., Dai,Q., Zheng,G., Yang,Y., Yi,C., Lindahl,T., Pan,T., Yang,Y.G. et al. (2011) N6-Methyladenosine in nuclear RNA is a major substrate of the obesity-associated FTO. *Nat. Chem. Biol.*, **7**, 885–887.
27. Kierzek,E. and Kierzek,R. (2003) The thermodynamic stability of RNA duplexes and hairpins containing N6-alkyladenosines and 2-methylthio-N6-alkyladenosines. *Nucleic Acids Res.*, **31**, 4472–4480.